SSRG International Journal of Electrical and Electronics Engineering
ISSN: 2348-8379/ https://doi.org/10.14445/23488379/IJEEE-V11I6P125

Volume 11 Issue 6, 234-241, June 2024

Original Article

Optimizing Targeted Drug Delivery Using LSTM and TLR-Enhanced Molecular Communication in Cancer Therapy

Ashwini Katkar[1], Vinitkumar Dongre[2]

[1,2]*Department of Electronics and Telecommunication Engineering, Thakur College of Engineering and Technology, Mumbai University, Maharashtra, India.*

[1]*Corresponding Author : ashwini.katkar@vcet.edu.in*

Received: 12 April 2024 Revised: 14 May 2024 Accepted: 11 June 2024 Published: 29 June 2024

Abstract - *In cancer treatment, the continuous aim is to find innovative solutions that effectively target malignant cells while limiting harm to healthy tissues. Molecular Communication (MC) has developed as a promising approach for targeted drug delivery, but congestion issues often hamper it. This study introduces a novel framework that combines Long Short-Term Memory (LSTM) congestion control with Toll-Like Receptor (TLR) feedback mechanisms to enhance drug delivery efficiency in cancer therapy. Using COMSOL simulations to determine congestion angles, LSTM models are trained, giving an accuracy rate of 97.75%. Through extensive computational modeling, the proposed approach significantly reduces congestion and improves the targeting and elimination of cancer cells. This research represents a key advancement in cancer treatment, enabling the precise, safe, and efficient delivery of drugs directly to cancer cells.*

Keywords - *Cancer cell, Drug delivery, LSTM, Molecular Communication, Targeted drug.*

1. Introduction

The evolving landscape of cancer treatment demands innovative strategies that precisely target malignant cells while reducing damage to healthy tissues. Traditional therapeutic approaches often suffer from systemic effects, leading to undesirable side effects where the minute fraction of drugs (0.1%) is absorbed by the tumor while the vast majority (99.9%) disperses into healthy tissues [1]. Conventional chemotherapy accounts for 27% of cancer patient deaths [2].MC has developed as a promising solution for precise and minimally invasive targeted drug delivery. However, to fully realize the potential of MC in cancer therapy, it is crucial to address the significant congestion challenge.

This study introduces a novel framework for congestion control in MC-based cancer drug delivery, utilizing a dynamic model with LSTM-based adaptive control and a feedback system driven by TLR biomarkers. This allows for dynamic adjustments to the number of drug molecules transmitted, effectively preventing congestion and ensuring optimal drug delivery for the successful eradication of cancer cells. The significance of this study lies in its comprehensive approach to addressing drug congestion in cancer therapy. Firstly, the dynamic model with LSTM control facilitates transmission rate adaptation. Secondly, the feedback loop provides a precise and instantaneous indicator of receptor availability, thereby enhancing the system's responsiveness and efficacy.

Through computational modeling, this research aims to demonstrate the exceptional potential of TLR-guided, LSTM-controlled MC for targeted cancer drug delivery. The successful implementation of this framework promises to revolutionize cancer treatment by providing a safe, precise, and effective method for delivering medications directly to their intended targets. The major findings of this work are given below:

- It proposes a dynamic model for MC with LSTM congestion control and TLR feedback for delivering drugs specifically to cancer cells.
- Using COMSOL simulations to determine congestion angles, LSTM models are trained, giving an accuracy rate of 97.75%.

Following this introduction, Section 2 specifies a review of the literature on congestion in MC and targeted drug delivery. Section 3 describes the mathematics of molecular communication in cancer treatment. Next, Section 4 illustrates the methodology. Section 5 shows the simulation results. Section 6 provides the conclusion and explores potential future research directions.

Figure 1 illustrates the fundamental principle of the dynamic model for molecular communication featuring LSTM congestion control. The transmitter initiates the release of drug molecules, which traverse a medium, such as body fluid, to reach the intended receiver, for instance, a cancer cell.

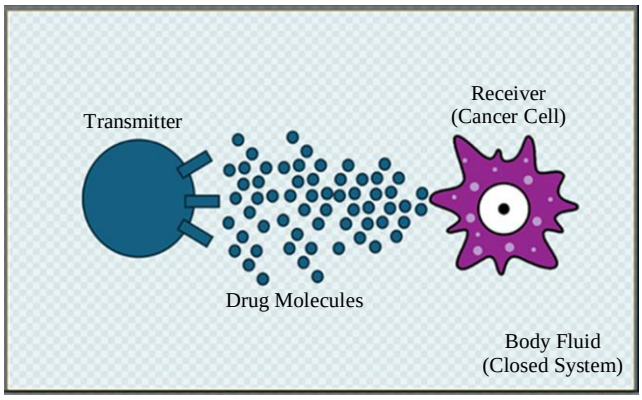

Fig. 1 The fundamental principle of a drug delivery model based on molecular communication

2. Related Literature

In the realm of targeted drug delivery to cancer cells, recent advancements have witnessed the convergence of molecular communication, advanced control mechanisms, and feedback systems. This survey examines the key components and contributions of this dynamic model, illuminating its significance within the broader landscape of molecular communication and targeted drug delivery research. Nakona et al. [3] explored the throughput and efficiency aspects of molecular communication. The authors evaluated an optimum transmission rate where efficiency was found to be 4%.

Felicetti et al. [4] suggested a connection-oriented protocol that employs TCP-like probing to identify an optimal transmission rate between the transmitter and receiver, thereby preventing receiver congestion. A delivery efficiency of 20 to 30% is achieved through a transmission rate adaptation technique. This technique adjusts the transmission rate based on the congestion detected at the receiver, ensuring optimal transmission performance.

Another study by Felicetti et al. [5] focuses on controlling the release rate in molecular communication to ensure target cells receive an accurate quantity of drug within a specified period, minimizing probable side impacts. Their techniques are validated through an extensive simulation, providing insights into delivery efficiency and time. Drug delivery efficiency of 25-35% was achieved using rate adaptation techniques. The primary contribution of Femminella et al. [6] lies in an examination of the factors causing congestion in MC systems. The findings of this study can be utilized in rate control algorithms to find the release rate of molecules effectively. This involves simultaneously managing the growth of both populations of cancer cells through the action of drugs, and detrimental toxic side effects on healthy cells.

Alam et al. [7] developed a transport layer protocol for body area nanonetworks, aiming to optimize network performance metrics to achieve desired levels of performance while minimizing complexity and overhead. The protocol has a steady delivery efficiency of around 20%. Salehi et al. [8] characterized a molecular communication channel based on diffusion involving interactions between ligands and receptors within a probabilistic absorber. The concentration is 20% to 35% in a fully absorbing receiver compared to the scenario with a partially absorbing receiver for 1D. Sharifi et al. [1] address the challenge of reducing channel uncertainties in tactile MC for immuno-chemotherapy with precise drug targeting. They introduced a revised tumor-immune interaction model that accounts for the stochastic nature of drug concentration at the tumor location. Within the realm of MC, this method is viewed as more resilient for transmitting information and integrating feedback.

Sohrabi et al. [9] investigate the targeted delivery of functionalized Carbon Nanotubes (CNTs) by traversing the lung cell membrane. Error, flow control, and the application of Shannon's theorem are utilized for developing a comprehensive digital communication system that models gene expression. Zhao et al. [10] compute and enhance the drug release rate of nanomachines by using an approach that involves queuing and a response model based on diffusion channels to optimize the drug delivery process. The optimum release rate reported for a single nanomachine is 63 molecules per microsecond. When multiple nanomachines are involved, the total is calculated by summing the positions of all nanomachines relative to the receptor position.

Sun et al. [11] propose a collaborative MC system designed for drug delivery, where the system incorporates a self-adaptive concentration gradient field search algorithm and a biosensor to offer secondary feedback. Tania et al. [12] in their study explore simultaneous drug delivery within MC-based targeted drug delivery systems by incorporating internal controllers. It employs a multi-objective optimization framework aimed at maximizing drug delivery efficiency while minimizing the time required for drug delivery. The proposed schemes enhance the number of drug doses by around 30 times.

Iqbal et al. [13] highlight miR34a's role as a key controller of tumor suppressor genes. The review presented by Hong et al. [14] focuses on advancements in research related to several receptors on cancer cells. They also described the development of unique nano-systems for targeted delivery of anticancer drugs to these cell surfaces. Wang et al. [15] describe extracellular vesicles as the biogenesis and explore their roles in cancer and outline therapeutic applications as an innate delivery mechanism in cancer treatment. Damrath et al. [16] formulated an analytical solution to simulate the monitored release of drugs. The quasiconvex/quasiconcave nature of a bilevel optimization problem has been

demonstrated and verified. Shafer et al. [17] explored approaches for targeting cancer cells involving endogenous and exogenous responsive systems, as well as the latest advancements in drug delivery methods. They examined how the carrier transmitter responds to a receiver located within the channel. Varshney et al. [18] discuss the challenges in utilizing TLR7/8 agonists for cancer therapy due to issues with solubility and toxicity.

However, biomaterial-based drug delivery systems offer a promising avenue to address these limitations and enhance the efficacy of TLR7/8 agonists in cancer treatment. Birkan et al. [19] utilize the artificial neural networks technique to model the received signal for a spherical transmitter. The authors demonstrate the utilization of a convolutional neural network for demodulation, which exhibits a superior performance of 5.5 bits/sec compared to the conventional approach.

The literature reviewed points out significant advancements in targeted drug delivery within the realm of MC. However, despite these strides, there exists a notable gap concerning congestion management within MC systems, particularly in the context of enhancing drug delivery efficiency for cancer therapy. While various studies have addressed aspects such as transmission rate adaptation, release rate control, and channel characterization, there remains a lack of comprehensive frameworks that effectively tackle congestion issues to optimize drug delivery. This study aims to fill this gap by introducing a novel framework that integrates Long Short-Term Memory (LSTM) congestion control with Toll-Like Receptor (TLR) feedback mechanisms. By leveraging COMSOL simulations to identify congestion angles and training LSTM models with high accuracy rates, this approach promises to enhance drug delivery efficiency in cancer therapy, offering a more robust solution to address congestion challenges in MC-based targeted drug delivery systems.

3. Mathematics of Molecular Communication in Cancer Cell

The following concept is used for creating geometry of transmitter (drug source) and receiver (cancer cell) in COMSOL implementation. Consider an asymmetric cancer cell with radius as mean radius and max radius. The average radius of Cancer cells is given by Equation 1,

$$Avg\ Radcc = \frac{Radius\ Mean + Radius\ Max}{2} \quad (1)$$

Figure 2 shows the schematic showing the cancer cell, the drug molecule attached to the cancer cell, and the average radius of the cell is Avg. $Rad_{cc.}$ Toll-Like Receptors (TLRs) are shown on cancer cells. TLRs are proteins that detect pathogens and trigger immune responses. Specifically, TLR7 and TLR8 can serve as novel diagnostic biomarkers, indicators of tumor progression and prognosis, and targets for immunotherapy in various cancers [20].

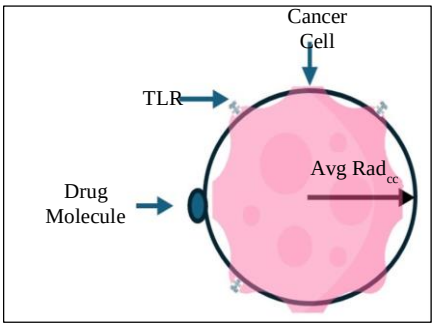

Fig. 2 The schematic of the cancer cell, drug molecule attached to the cancer cell and average Rad_{cc}

Therefore, volume is given by Equation 2,

$$Volume = \frac{4}{3}\pi(Avg\ Rad_{cc})^3 \quad (2)$$

The approximation of cancer is huge compared to drug molecules.

Molecule Rad= R_{Mol} and Rint=R_{Mol}

Figure 3 shows the schematic to define the region of intersection of molecules with cancer cells depicted by Rint.

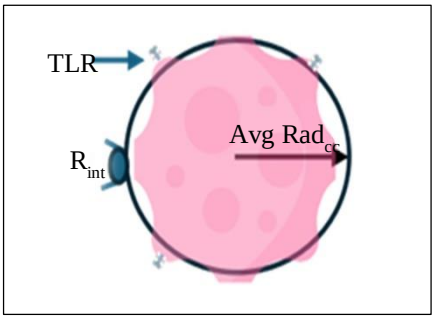

Fig. 3 Schematic to define the region of intersection of molecules with cancer cells depicted by Rint

Molecules in a 2D environment are approximated as given in Equation 3,

$$Molecule\ in\ 2D = \frac{Perimeter}{RMol} \quad (3)$$

i.e.

$$Molecule\ in\ 2D = \frac{2\pi\ (Avg\ Radcc)}{RMol} \quad (4)$$

It is assumed that cells are symmetric in all directions. The 2D simulation will be valid for 3D real-world applications. Molecules in a 3D environment are approximated as given in Equation 5,

$$Molecule\ in\ 3D = \pi(Molecule\ in\ 2D) \quad (5)$$

As the surface area of a sphere is given by Equation 6,

$$Surface\ area\ of\ sphere = 4\pi r^2 \quad (6)$$

Cross section area is given by Equation 7 as,

$$Cross\ section\ area\ of\ sphere = \pi R_{Mol}^2 \quad (7)$$

Figure 4 Schematic depicting cancer cells in 3D surrounded by drug molecules.

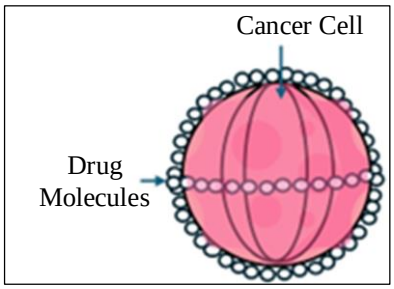

Fig. 4 Schematic of cancer cell in 3D surrounded by molecules

The actual area is transformable in 3D. It is assumed that the cells are symmetric in all directions. Hence, any 2D simulation will be valid for 3D real-world applications. Thus, drug molecules in a 3D environment are given by Equation 8,

$$Molecule\ in\ 3D = \frac{4\pi Avg\ Radcc}{\pi(Rmol)^2} \quad (8)$$

Congestion occurs when all transmitted molecules reaching the receiver are equal to Molecules in 3D (M3D).

Let Ra be the rate of arrival and Rab is the rate at which the molecule is absorbed. The rate of absorption of molecules is less than the arrival. Also, throughput, i.e. number of molecules successfully received per unit of time, is directly proportional to Ra.

Let R_{Rtx} be the number of molecules released per second when there is no diffusion. Figure 5 shows the schematic diagram showing molecules traveling from transmitter to receiver with the rate of release of molecules defined by RRtx.

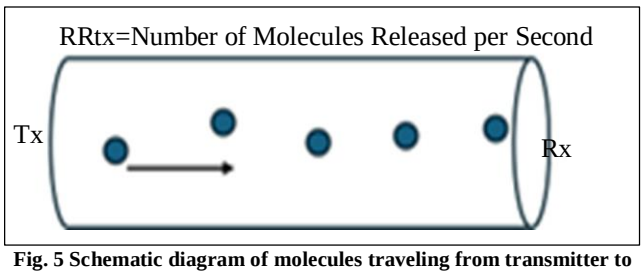

Fig. 5 Schematic diagram of molecules traveling from transmitter to receiver with the rate of release of molecules defined by RRtx

The number of released molecules will be equal to the rate of arrival of molecules as given by Equation 9,

$$\text{RRtx} = Ra \quad (9)$$

But practically, the rate of release of molecules by the transmitter is always greater than the rate of arrival, given by Equation 10, as

$$RRTx > Ra \quad (10)$$

Now, let molecules diffuse through the surroundings to reach the receiver. The diffusion coefficient is given by Equation 11,

$$D = \frac{4KbT}{6\pi\eta R} \quad (11)$$

Kb= Boltzmann Constant, given by,

$$Kb = 1.38 * 10^{-23}\frac{J}{K}$$

T= Absolute Temperature in degrees Kelvin
η = Viscosity of the fluid (3.5 to 4.5 centipoises for blood)
R= Radius of propagating molecules.

The number of molecules received at the receiver is given by Equation 12,

$$\mathrm{R_{RX}} = \frac{\mathrm{R_{TX}} e^{-\left(\frac{d^2}{4Dt}\right)}}{\sqrt{4\pi Dt}} \quad (12)$$

Figure 6 illustrates the concept of a molecular communication channel, showcasing the interaction between a transmitter (represented by a drug molecule) and a receiver (depicted as a cancer cell).

The maximum distance a particle must travel to reach the backside of cancer cell TLR at 180 degrees is the maximum distance, Dmax. The direct path, depicted as a solid line, symbolizes the ideal trajectory for the drug molecule to reach its intended target.

Dotted lines, on the other hand, represent potential diffusion paths that drug molecules may follow due to factors such as Brownian motion or other interactions within the biological environment. These alternative routes have the potential to lead to delayed delivery or reduced drug concentration at the target site. Furthermore, obstacles or barriers within the environment are also depicted in the image, demonstrating how they might hinder the direct path of the drug molecules.

$$Dmax = (d - \Delta n) + \frac{2\pi Avg\ Radcc + \Delta n}{2} \quad (13)$$

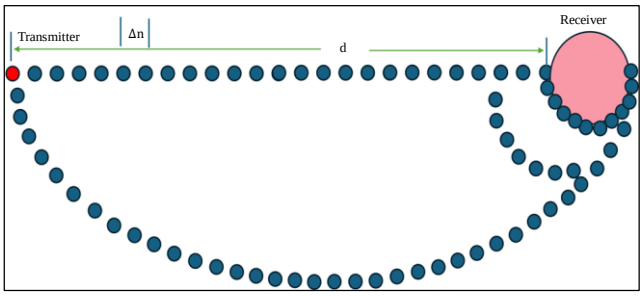

Fig. 6 A molecular communication channel with potential diffusion paths in targeted drug delivery

4. Methodology

The methodology employed in this study outlines the development and evaluation of a molecular communication system tailored for targeted drug delivery to cancer cells. COMSOL simulation environment is used to replicate the flow characteristics within the targeted drug delivery system. The values obtained from the COMSOL simulation are plugged into the Python code for LSTM implementation. At the core of this system are innovative strategies, such as LSTM congestion control and feedback mechanisms, strategically implemented to optimize both drug delivery efficiency and the cancer kill rate. The system's dynamic model plays a pivotal role in this optimization process, continuously adapting the number of drug molecules based on the feedback.

4.1. COMSOL Simulation

The methodology in this work utilized COMSOL multiphysics, a versatile computational platform, for simulation study. Laminar flow was modeled within the COMSOL environment to replicate the flow characteristics within the targeted drug delivery system. The built-in laminar flow module simulates the fluid behavior, ensuring an accurate representation of the transport phenomena. The simulation parameters are defined in Table 1.

Figure 7 illustrates a COMSOL multiphysics particle tracking simulation depicting various stages of drug delivery over time. At t = 3 sec (a), drug molecules, or particles, begin emitting in all directions equally, marking the early phase where particles are just released from the targeted drug delivery system. In (b) at t = 6 sec, particles continue to move uniformly. By (c) at t = 9 sec, particles gradually alter their trajectory towards cancer cells within the closed system simulation, unable to persistently move away from the cancer cells.

By (d) at t = 12 sec, particles reorient to attack cancer cells. (e) at t = 15 sec, drug molecules initially following a straight path contact the cancer cell surface. By (f) at t = 25 sec, particles have begun to saturate. In (g) at t = 35 seconds, more than half of the cancer cell is occupied by congested drug molecules. However, achieving congestion on the backside of the cell remains challenging due to the cell's rotation, even as drug molecules already occupy all attractors on the front side. This time-dependent congestion progression presents an intriguing observation.

Table 1. COMSOL multiphysics simulation parameters

S. No.	Description	Value
1	Flow Rate	3E−10 m³/s
2	Particle Density	1300 kg/m³
3	Minimum Particle Diameter	1.5E−6 m
4	Maximum Particle Diameter	1.1E−5 m
5	Length of inlets	0.6 (mm)
6	Width of Inlets	0.1 (mm)
7	The Angle between Two Inlets	60 (deg)
8	Length of Micro-Channel	140 (um)
9	Width of Micro-Channel	20 (um)
10	Flow Type	Laminar
11	Temperature	310k

4.2. LSTM Implementation and TLR Feedback

Long Short-Term Memory (LSTM) represents a class of Recurrent Neural Network (RNN) architectures engineered to tackle the vanishing gradient issue encountered in conventional RNNs [21]. Leveraging specialized memory cells and gating mechanisms, LSTMs excel in capturing long-term dependencies within sequential data.

This selective memory capability empowers LSTMs to retain or discard information over time, rendering them highly proficient in tasks revolving around sequential data, including time, series forecasting, natural language processing, and speech recognition.

To mitigate the challenge of congestion, the LSTM function is applied, selectively activating congestion control only when a predefined threshold is surpassed. This ensures a novel approach to congestion management, allowing the system to maintain efficiency without compromising its effectiveness.

This study focused on predicting future values of time series data employing an LSTM model. Python served as the programming language, while TensorFlow served as the framework for constructing and training the model. Additionally, numpy, pandas, and matplotlib libraries were utilized for data manipulation and visualization purposes.

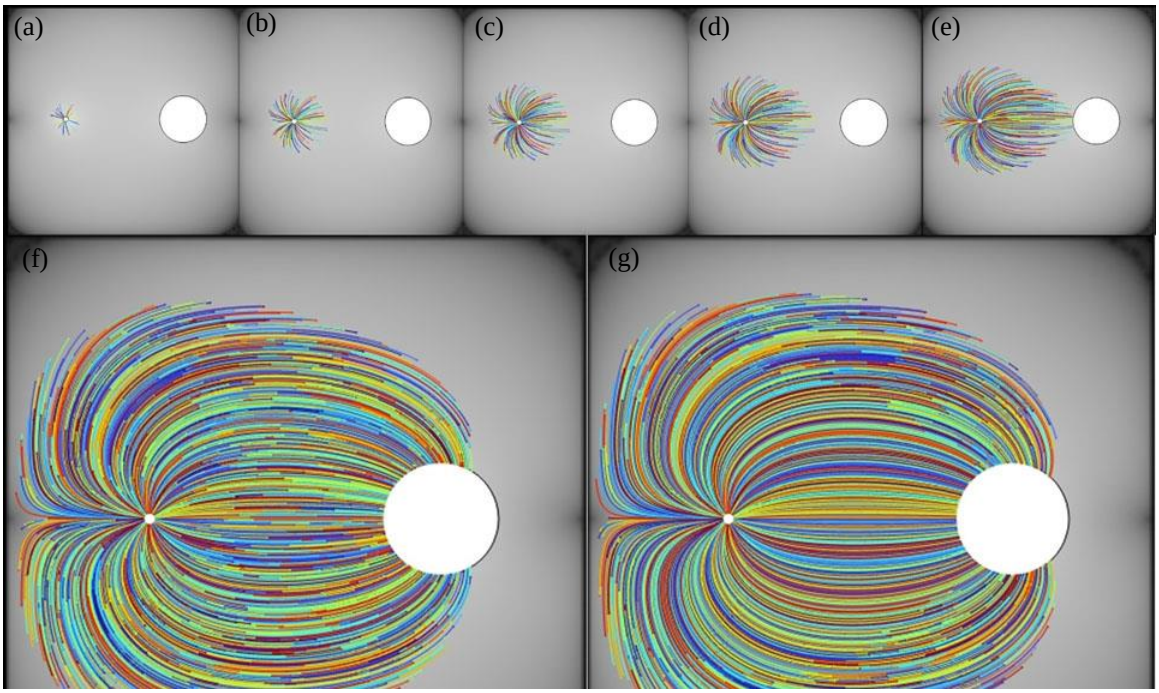

Fig. 7 COMSOL multiphysics particle tracking simulation at different time points (a) at t = 3 sec, (b) at t = 6 sec, (c) at t = 9 sec, (d) at t = 12 sec, (e) at t= 15 sec, (f) at t = 25 sec, and (g) at t = 35 seconds.

4.2.1. Data

The data we used was a tab-separated text file containing two columns: x and y. The x column represented the time steps from 1 to 99, and the y column represented the corresponding values of the time series. The data was provided by the instructor and had the following characteristics:

- The data had a non-linear trend and a seasonal pattern.
- The data had a minimum value of 0 and a maximum value of 271.85.
- Data is split into lines and then into columns using the Python built-in functions strip () and split (). In the next step, the lists of x and y values are converted into numpy arrays using the np. array () function.

4.2.2. Data Preprocessing

The data is normalized using the min-max normalization technique, which scales the data to the range of 0 to 1. Following Equation 14 is used to normalize the data:

$$xnorm = \frac{x - xmin}{xmax - xmin} \quad (14)$$

Where x_{norm} is the normalized value, x is the original value, x_{min} is the minimum value, and x_{max} is the maximum value of the data.

The formula was applied to both the x and y arrays using numpy operations. The data was then reshaped for LSTM using the reshape () function. The x array was reshaped into a three-dimensional array of shapes (99, 1, 1), where 99 represents the number of samples, 1 represents the number of time steps, and 1 represents the number of features. The y array was reshaped into a two-dimensional array of shapes (99, 1), where 99 is the number of samples, and 1 is the number of features.

4.2.3. Model

An LSTM model was built using the Sequential class from the TensorFlow Keras API. Two layers were added to the model: an LSTM layer and a dense layer. The LSTM layer had 50 units and took the input shape of (1, 1). The dense layer had one unit and used the default linear activation function. The model was compiled using the Adam optimizer and Mean Squared Error (MSE) as the loss function.

4.2.4. Training

The model was trained until the maximum predicted value reached 360, or the number of epochs reached 400, whichever occurred first. A batch size of 1 and a verbose level of 2 were used. The epoch number and the maximum predicted value were printed after each epoch. Additionally, the Mean Squared Error (MSE) of the model on the training data was calculated and printed after the training was completed.

4.2.5. Prediction

Predictions were generated using the model on the normalized x array. Subsequently, the predictions were denormalized using the inverse of the min-max normalization Equation 15,

$$x = [xnorm * (xmax - xmin)] + xmin \qquad (15)$$

Where x is the denormalized value, xnorm is the normalized value, xmin is the minimum value, and xmax is the maximum value of the data.

The formula was applied to the predictions array using numpy operations. The true and predicted values of the time series were then plotted using the matplotlib library, with the true values labeled as 'True' and the predicted values labeled as 'Predicted'.

5. Results and Discussion

Figure 8 illustrates the output of the COMSOL simulation. It can be observed that the initial congestion angle remains at zero for approximately 15 seconds. After this period, it grows exponentially before gradually transitioning towards slow saturation.

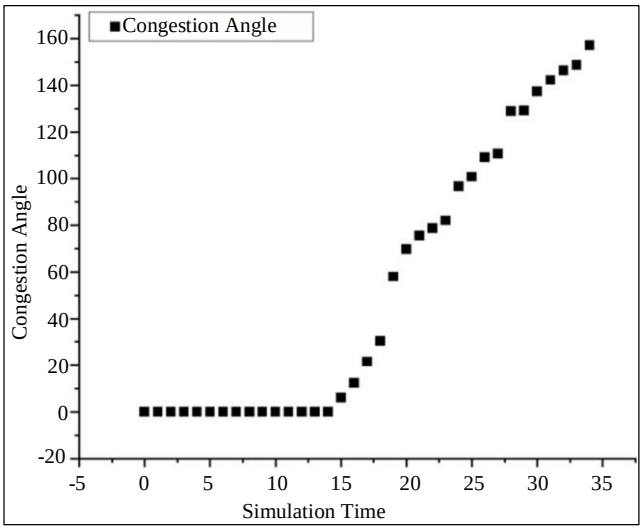

Fig. 8 Plot of simulation time vs congestion angle

Figure 9 displays the output curve of LSTM predictions on the congestion angle compared to the true congestion observed in degrees by the closed-loop system. It is evident that while the prediction may be accurate for the latter half of the curve, the initial flat region is not accurately predicted by the LSTM.

The LSTM erroneously predicts negative congestion angles, which are practically impossible, suggesting the potential for correction in the LSTM curve. The error in the initial iterations is substantial, but as the number of simulations exceeds 50, the accuracy significantly improves.

Integrating LSTM-based adaptive control and TLR feedback mechanisms within the molecular communication framework offers a novel strategy to enhance targeted drug delivery efficiency. The system's adaptability to the evolving landscape of cancer cells is demonstrated by dynamically adjusting drug molecule release based on real-time TLR values.

The LSTM congestion control mechanism provides a novel approach by selectively activating congestion control when predefined thresholds are exceeded. This ensures efficient drug delivery without compromising effectiveness, maximizing therapeutic outcomes while minimizing adverse effects.

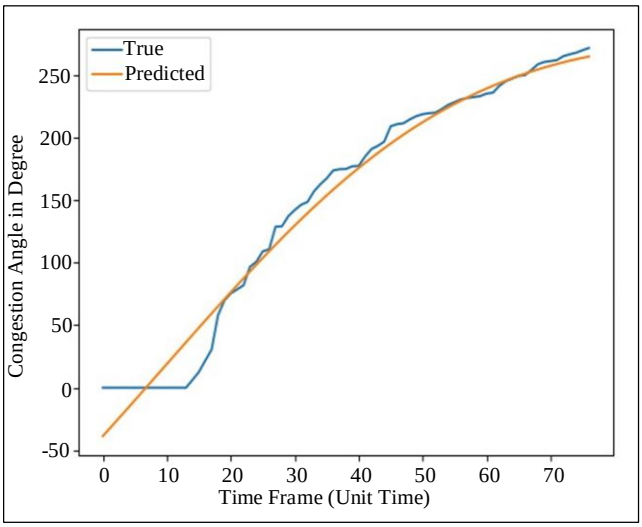

Fig. 9 The output curve of LSTM prediction on congestion angle and true congestion observed by the close loop system. It was clear that prediction may be accurate for the later half of the curve, but the initial flat region is not predicted by LSTM.

6. Conclusion

The dynamic model proposed in this study for molecular communication with LSTM congestion control and TLR feedback offers a comprehensive framework to enhance precise drug delivery to cancer cells. This research addresses the critical challenge of congestion in MC-based cancer therapy by integrating innovative control mechanisms and feedback systems. By dynamically adjusting the number of drug molecules transmitted based on real-time TLR values, the system adapts to the fluctuating environment of cancer cells.

The LSTM congestion control mechanism allows for congestion management, ensuring efficient drug delivery without compromising effectiveness with an accuracy of 97.75%, with error reduction as training iterations increased. By selectively activating congestion control when predefined thresholds are surpassed, the system maximizes therapeutic outcomes while minimizing adverse effects.

In future research, further refinement and optimization of the LSTM algorithm, improvements in TLR detection technology, and scaling the proposed framework for clinical applications could enhance the model's robustness and applicability.

References

[1] Neda Sharifi et al., "Overcoming Channel Uncertainties in Touchable Molecular Communication for Direct-Drug-Targeting-Assisted Immuno-Chemotherapy," *IEEE Transactions on NanoBioscience*, vol. 19, no. 2, pp. 249-258, 2020. [CrossRef] [Google Scholar] [Publisher Link]

[2] Dipak D. Gadade et al., "Strategies for Cancer Targeting: Novel Drug Delivery Systems Opportunities and Future Challenges," *Targeted Cancer Therapy in Biomedical Engineering*, pp. 1-42, 2023. [CrossRef] [Google Scholar] [Publisher Link]

[3] Tadashi Nakano, Yutaka Okaie, and Athanasios V. Vasilakos, "Throughput and Efficiency of Molecular Communication between Nanomachines," *2012 IEEE Wireless Communications and Networking Conference (WCNC)*, Paris, France, pp. 704-708, 2012. [CrossRef] [Google Scholar] [Publisher Link]

[4] Luca Felicetti et al., "TCP-Like Molecular Communications," *IEEE Journal on Selected Areas in Communications*, vol. 32, no. 12, pp. 2354-2367, 2014. [CrossRef] [Google Scholar] [Publisher Link]

[5] Luca Felicetti, Mauro Femminella, and Gianluca Reali, "Congestion Control in Molecular Cyber-Physical Systems," *IEEE Access*, vol. 5, pp. 10000-10011, 2017. [CrossRef] [Google Scholar] [Publisher Link]

[6] Mauro Femminella, Gianluca Reali, and Athanasios V. Vasilakos, "A Molecular Communications Model for Drug Delivery," *IEEE Transactions on NanoBioscience*, vol. 14, no. 8, pp. 935-945, 2015. [CrossRef] [Google Scholar] [Publisher Link]

[7] Mayisha Alam et al., "Conjugate Congestion Control Based Transport Layer Protocol for Molecular Communication in Body Area Nanonetworks (BANs)," *2018 5th International Conference on Networking, Systems and Security (NSysS)*, Dhaka, Bangladesh, pp. 1-6, 2018. [CrossRef] [Google Scholar] [Publisher Link]

[8] Shirin Salehi, Naghmeh S. Moayedian, and Eduard Alarcón, "Diffusion-Based Molecular Communication Channel in Presence of a Probabilistic Absorber: Single Receptor Model and Congestion Analysis," *IEEE Transactions on NanoBioscience*, vol. 18, no. 1, pp. 84-92, 2019. [CrossRef] [Google Scholar] [Publisher Link]

[9] Nafiseh Sohrabi et al., "Analysis of Dynamics Targeting CNT-Based Drug Delivery through Lung Cancer Cells: Design, Simulation, and Computational Approach," *Membranes*, vol. 10, no. 10, pp. 1-16, 2020. [CrossRef] [Google Scholar] [Publisher Link]

[10] Qingying Zhao, Min Li, and Lin Lin, "Release Rate Optimization in Molecular Communication for Local Nanomachine-Based Targeted Drug Delivery," *IEEE Transactions on NanoBioscience*, vol. 20, no. 4, pp. 396-405, 2021. [CrossRef] [Google Scholar] [Publisher Link]

[11] Yue Sun et al., "A Cooperative Molecular Communication for Targeted Drug Delivery," *Bio-inspired Information and Communication Technologies*, pp. 16-26, 2020. [CrossRef] [Google Scholar] [Publisher Link]

[12] Tania Islam, Ethungshan Shitiri, and Ho-Shin Cho, "A Molecular Communication-Based Simultaneous Targeted-Drug Delivery Scheme," *IEEE Access*, vol. 9, pp. 96658-96670, 2021. [CrossRef] [Google Scholar] [Publisher Link]

[13] Muhammad Javed Iqbal et al., "Targeted Therapy Using Nanocomposite Delivery Systems in Cancer Treatment: Highlighting miR34a Regulation for Clinical Applications," *Cancer Cell International*, vol. 23, pp. 1-12, 2023. [CrossRef] [Google Scholar] [Publisher Link]

[14] Liquan Hong et al., "Nanoparticle-Based Drug Delivery Systems Targeting Cancer Cell Surfaces," *RSC Advances*, vol. 13, no. 31, pp. 21365-21382, 2023. [CrossRef] [Google Scholar] [Publisher Link]

[15] Li Wang et al., "Extracellular Vesicles for Drug Delivery in Cancer Treatment," *Biological Procedures Online*, vol. 25, pp. 1-15, 2023. [CrossRef] [Google Scholar] [Publisher Link]

[16] Martin Damrath et al., "Optimization of Extracellular Vesicle Release for Targeted Drug Delivery," *IEEE Transactions on NanoBioscience*, vol. 23, no. 1, pp. 109-117, 2023. [CrossRef] [Google Scholar] [Publisher Link]

[17] Maximilian Schäfer et al., "Channel Responses for the Molecule Release from Spherical Homogeneous Matrix Carriers," *IEEE Transactions on Molecular, Biological and Multi-Scale Communications*, vol. 8, no. 4, pp. 212-228, 2022. [CrossRef] [Google Scholar] [Publisher Link]

[18] Dhruv Varshney et al., "Employing Drug Delivery Strategies to Overcome Challenges Using TLR7/8 Agonists for Cancer Immunotherapy," *The AAPS Journal*, vol. 23, 2021. [CrossRef] [Google Scholar] [Publisher Link]

[19] H. Birkan Yilmaz et al., "A Machine Learning Approach to Model the Received Signal in Molecular Communications," *2017 IEEE International Black Sea Conference on Communications and Networking (BlackSeaCom)*, Istanbul, Turkey, pp. 1-5, 2017. [CrossRef] [Google Scholar] [Publisher Link]

[20] Hao Sun et al., "Targeting Toll-Like Receptor 7/8 for Immunotherapy: Recent Advances and Prospectives," *Biomarker Research*, vol. 10, pp. 1-19, 2022. [CrossRef] [Google Scholar] [Publisher Link]

[21] Sepp Hochreiter, and Jürgen Schmidhuber, "Long Short-Term Memory," *Neural Computation*, vol. 9, no. 8, pp. 1735-1780, 1997. [CrossRef] [Google Scholar] [Publisher Link]